

Substitution of a Chlorophyll into the Inactive Branch Pheophytin-Binding Site Impairs Charge Separation in Photosystem II

Ling Xiong,[†] Michael Seibert,[‡] Alexey V. Gusev,[§] Michael R. Wasielewski,[§] Craig Hemann,^{||} C. Russ Hille,^{||} and Richard T. Sayre^{*,†}

Departments of Plant Cellular and Molecular Biology and Molecular and Cellular Biochemistry, Ohio State University, Columbus, Ohio 43210, National Renewable Energy Laboratory, Golden, Colorado 80401, and Department of Chemistry, Northwestern University, Evanston, Illinois 60208

Received: March 31, 2004

All photosynthetic reaction centers (RCs) have two parallel sets of electron transfer cofactors that cross the membrane. In quinone-type RCs (including photosystem II (PSII)), however, only one pathway (the active branch) is used for electron transfer. Since the electron transfer cofactors of each pathway have nearly identical distance and orientation relationships, it is assumed that local differences in protein environment determine the directionality of electron transfer. To understand further the factors that affect energy distribution among the PSII RC cofactors, we altered the PSII RC cofactor symmetry by replacing the inactive-branch pheophytin (Pheo) with a chlorophyll (Chl). We mutated the D1-L210 residue to a histidine (D1-L210H) to provide a Mg ligand for Chl. Analyses of the pigment composition of D1-L210H RCs indicated that the inactive-branch Pheo had been replaced by a Chl. Comparisons of wild-type and D1-L210 transient absorption spectra confirmed that the red-shifted Pheo Q_x absorption band (543.5 nm) belonged to the active-branch Pheo. Surprisingly, intact D1-L210H PSII complexes were unable to evolve oxygen, lacked Chl variable fluorescence, (following a flash), and were unable to photoaccumulate reduced Q_A, indicating that electron transfer in D1-L210H PSII complexes was severely perturbed. The kinetics of primary charge separation, however, were not substantially altered in D1-L210H RCs, indicating that the Chl substitution had not perturbed the energetics of the primary electron donor/acceptor pair. Significantly, intact D1-L210H PSII core complexes had a substantially increased and red-shifted Chl fluorescence emission band attributed to fluorescence from Chl's of the distal antenna complex as well as a blue-shifted fluorescence emission peak attributed to Chl's of the proximal antenna complex (77 K). These results are interpreted in terms of a redistribution of the excited-state energy among the pigments of the RC multimer, leading to loss of the excited state via fluorescence in the D1-L210H mutant.

Introduction

Photosystem II (PSII)⁵¹ in plants and algae catalyzes the light-driven oxidation of water and reduction of plastoquinone. Primary charge separation takes place in the reaction center (RC), consisting of the D1, D2, cytochrome *b*₅₅₉, and *psbI* proteins as well as six chlorophyll (Chl) and two pheophytin (Pheo) electron transport cofactors (Figure 1). The structural organization of the core pigments in PSII RCs is similar to that in the bacterial reaction center (BRC) of *Rhodospirillum rubrum*, and thus the BRC has served as an important model for PSII structure and function (for a review see refs 1–3). In both BRC and PSII RC complexes, electron transfer from the excited state of a primary donor Chl to a Pheo represents the primary photochemical event of photosynthesis. Reduced Pheo rapidly reduces a quinone bound at the Q_A-binding site in intact PSII preparations (Q_A⁻ is missing from isolated PSII RCs), generating the stable charge-separated state P⁺/Q_A⁻. In the intact PSII

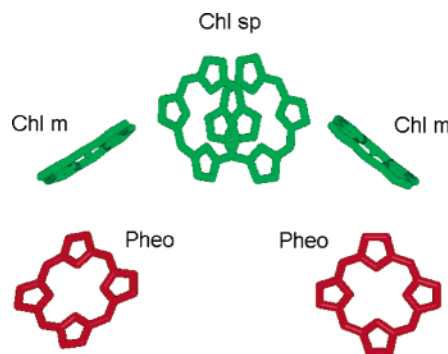


Figure 1. Structural arrangement of PSII coordinates according to Zouni et al.⁶ The phytyl tails are truncated for clarity.

complex, the oxidized primary donor Chl is reduced by electrons that are ultimately extracted from water in a process generating molecular O₂.

All quinone-type reaction centers (PSII and the BRC) have two parallel and C₂ symmetry-related electron transfer pathways that transcend the membrane (see Figure 1 for a schematic representation of the coordinates of the PSII RC).^{4–6} In the BRC, primary electron transfer occurs almost exclusively (90%) along the L-branch (active branch), one of two parallel electron transfer pathways.⁷ Similarly, charge separation in water-splitting PSII

* Corresponding author. Telephone: (614) 292-9030. Fax: (614) 292-6345. E-mail: sayre.2@osu.edu.

[†] Department of Plant Cellular and Molecular Biology, Ohio State University.

[‡] National Renewable Energy Laboratory.

[§] Northwestern University.

^{||} Department of Molecular and Cellular Biochemistry, Ohio State University.

complexes takes place along only the active branch.^{4,8} At present, the structural basis for this functional asymmetry in electron transfer is not apparent, due to the fact that the cofactors of both branches have nearly identical orientations and distances between adjacent cofactors. This similarity in structural orientation of the Chl's is associated with a lack of diagnostic spectral features, which might be used to differentiate the RC Chl's from each other. Similarly, the two Pheo's have nearly identical spectral features, even at cryogenic temperatures. Bleaching of the Pheo Qx bands (542 nm) and the primary donor (P680) Qy band are the only diagnostic optical transitions that are routinely used to monitor primary charge separation in PSII.^{9,10}

In the BRC the excited state, formed after light absorption, is trapped by the Chl's of the special pair (Chl_{SP}). Primary charge separation takes place between one Chl of the special pair and Pheo, and this is mediated by electron transfer through the active branch Chl monomer (for a review see refs 3 and 11). In contrast to the BRC, a substantial body of evidence indicates that the primary donor in PSII is a Chl monomer (Chl_M), located between the Chl_{SP} and the Pheo (Pheo_{active}) on the active branch.^{12–16} Furthermore, the excited state in PSII is not efficiently trapped by the Chl's of the Chl_{SP}, but rather is extensively delocalized across several pigments, including the Chl_{SP}, the two Chl_M's, and one or both of the Pheo's.^{10,17,18} This delocalization of the excited state across the core pigments of the PSII RC is known as the multimer model.¹⁷

While great progress has been made in characterizing the structural basis for the directionality of electron transfer and the identity of the primary donor Chl in the BRC,^{19–25} little is known about the structural or physical basis for primary charge separation in PSII. One approach that has been used to characterize the molecular basis for functional asymmetries in both the BRC and PSII is perturbation of the symmetry of the RC core cofactors by pigment substitution. In the BRC, Pheo's have been replaced with Chl's. This was achieved by providing an axial ligand for the Mg²⁺ ion of Chl by site-directed mutagenesis of amino acid residues that are located over the center of the Pheo macrocycle ring.^{21,22,26} One class of BRC RC pigment mutants that has been extensively characterized is the β -BRC mutants. The BPheo that participates in charge separation (BPheo_{active}) was replaced with a BChl in this group of mutants. The pigment substitution was achieved by replacing a leucine residue (M-L212 in *Rb. capsulatus* and M-L214 in *Rh. sphaeroides*) located near the center of the BPheo_{active} macrocycle ring with a histidine residue. The histidine residue provides a ligand for the Mg²⁺ ion of BChl, resulting in the replacement of the BPheo_{active} with a BChl.^{21,22} Extensive studies of β -type BRC mutants indicated that while charge separation occurs between P (the primary donor) and the BChl occupying the BPheo_{active} branch site, the quantum yield of the charge-separated state (P⁺Q_A⁻) was substantially reduced. This reduction in charge separation was associated with both an increased lifetime of P* (excited state) and an increased back reaction or charge recombination rate between P⁺ and BChl_L⁻.²¹ The reduction in the quantum yield of charge separation in these mutants was attributed to the greater reducing potential of BChl⁻ relative to BPheo⁻.

Recently, the two core Pheo's of PSII RCs have also been replaced with chemically modified Pheo's by detergent extraction, and pigment reconstitution approaches.^{27–30} Exogenous Pheo replaced approximately 100% of the Pheo_{inactive} and 40% of the Pheo_{active}. Resonance Raman studies of the modified PSII RCs indicated that the pigment substitution did not substantially alter the binding environment of the Pheo's or other cofactors.

However, circular dichroism (CD) spectral analyses indicated that both the wavelength and amplitude of the 681 nm positive peak were altered, as well as the negative chirality peak at 667 nm. These results indicated that the excitonic interactions between the core pigments were perturbed.

We have used a transgenic (site-directed mutagenesis) approach to modify the pigment composition of PSII RCs and to demonstrate that, by providing a ligand (D1-L210H) for a Chl Mg ion near the Pheo_{inactive} binding site, a Chl can be substituted for Pheo_{inactive}. The Pheo_{inactive} → Chl mutant forms stable RC complexes that can be isolated using standard protocols. However, intact mutant PSII complexes have a substantially impaired ability to evolve O₂ and do not accumulate reduced Q_A. The phenotype is attributed to an impaired ability to form a charge-separated state and to reduce Pheo_{active} in intact PSII (O₂-evolving) complexes. This impaired ability to form a charge-separated state is associated with a greatly increased level of Chl fluorescence emission measured at 77 K. These results are interpreted in terms of a redistribution of the excited-state equilibrium among the core pigments of the mutant RC, which leads to a reduced ability to trap the excited state and the increased Chl fluorescence. It is inferred that efficient charge separation in PSII is dependent upon properly biasing the distribution of excited states among the active branch pigments.

Material and Methods

Generating the D1-L210H Mutant. The nonconservative D1-L210H mutation was introduced into the chloroplast-encoded intron-less *psbA* gene present in plasmid PBA155.³¹ Codon 210 was changed from TTA to CAC by oligonucleotide directed mutagenesis leading to the substitution of the leucine residue with a histidine residue. The mutagenic oligonucleotide primers for the D1-L210H mutation were

5'-TTCGGTGGTTCAGCATTCTCAGCTATGCATGGT-
TCTT-3'

and

5'-TTCGGTGG TTCACACTTCTCAGCTATGCATGGT-
TCTT-3'

In addition, the D1-L210H mutagenic primers introduced a diagnostic *Nsi*I restriction endonuclease recognition site into the *psbA* gene by introducing a silent mutation at residue D1-H215. The plasmids containing mutagenized *psbA* fragments were transformed into the *Chlamydomonas reinhardtii* (*C. reinhardtii*) *psbA* deletion strain, CC 744, as described in ref 32. The preliminary identification of spectinomycin and streptomycin resistant transformants was performed by restriction site analysis of PCR-generated *psbA* fragments, followed by DNA sequencing using a standard DNA sequencing kit (Pharmacia). The control strain of *C. reinhardtii* used in our study is strain CC 2137 and is referred to as wild type (WT).

Isolation of PSII Particles. Control and mutant strains of *C. reinhardtii* were grown in Tris-acetate-phosphate (TAP) media at 25 °C in low light (5–15 μmol of photons $\text{m}^{-2} \text{s}^{-1}$) to avoid photoinhibition. Thylakoids and O₂-evolving PSII core particles of WT and the D1-L210H mutant were prepared from log-phase cells ruptured using a bionebulizer and solubilized with Triton X-100, respectively.³² The quality of the PSII RC particles was confirmed by the absence of a blue shift in the red maximum absorption peak prior to and after spectroscopic measurements.⁹ PSII RCs were prepared from PSII core particles

essentially as described in ref 33 with minor modifications. For removal of the proximal antenna complexes from D1-L210H mutant RCs, the TSK-DEAE-650 column was washed with buffer containing 0.2% (w/v) Triton X-100 rather than 0.35% Triton X-100 used for washing WT RCs. The Triton X-100 detergent was then exchanged with 2.0 mM η -dodecyl β -D-maltoside in Tris·HCl buffer containing 10% glycerol, pH 7.5, to stabilize the RCs. RCs were eluted in the n -dodecyl β -D-maltoside containing buffer with 150 mM NaCl. The relative amounts of Chl *a*, Pheo *a*, and carotenoids in the purified PSII RC complex were calculated according to ref 34 and confirmed by HPLC analysis (data not shown).

Biochemical and Biophysical Characterization of Wild-Type and Mutant PSII Complexes. Light-saturated ($1000 \mu\text{mol of photons m}^{-2} \text{s}^{-1}$) rates of O_2 evolution were measured as previously described in ref 32 using DMBQ (2,5-dimethyl-*p*-benzoquinone) as an electron acceptor. Room-temperature absorption spectra of PSII RCs were recorded using a Cary 3E UV–Vis spectrophotometer in buffer containing 50 mM Tris·HCl, pH 7.2, 10% glycerol (w/v), and 2.0 mM n -dodecyl β -D-maltoside at a Chl concentration of $5 \mu\text{g}$ of Chl/mL. Flash-induced microsecond Chl *a* fluorescence decay kinetics were measured using a pulse-modulated fluorometer as described by ref 35. Intact cells were diluted with TAP medium to a concentration of $20 \mu\text{g}$ of Chl/mL and incubated in the dark for 5 min prior to measurement.

X-band EPR spectra were recorded with a Bruker ESP-300 spectrometer equipped with an Oxford Instruments helium cryostat and temperature controller. For the detection of the $\text{Q}_\text{A}^- \text{Fe}^{2+}$ signal, PSII membranes were illuminated at 200 K for 10 min in the presence of 100 mM sodium formate to block Q_A -to- Q_B electron transfer. All samples were scanned 10 times. The signals were normalized on the basis of the $\text{Tyr}_\text{D}^{\bullet}$ signal. For light-induced generation of Pheo $^-$ signal, PSII RC preparations were illuminated in the presence of sodium dithionite (2 mg/mL) for 3 min at 4 °C by a white light source through a heat-absorbing filter, and rapidly frozen in 77 K for EPR measurements. The instrument settings were the following: sample temperature, 4 K; microwave power, 32 mW; microwave frequency, 9.48 GHz; field modulation frequency, 100 kHz; magnetic field modulation amplitude, 2.0 mT.

Light-induced absorption difference spectra using PSII RCs were recorded using an HP-8452a spectrophotometer. PSII RC preparations ($\sim 4.8 \mu\text{M}$ Chl) were suspended in buffer A supplemented with sodium dithionite (2 mg/mL) and 1 μM methyl viologen, and incubated in the dark at 4 °C for 5 min prior to measurement. To photoaccumulate reduced Pheo, the sample was illuminated with white light ($2800 \mu\text{mol of photons m}^{-2} \text{s}^{-1}$) for 10 s prior to measurements. Samples were kept at 4 °C with a circulated refrigerated water bath during data collection.

Steady-state 77 K Chl fluorescence emission spectra of PSII preparations were recorded on a Fluoro-Max spectrometer with a homemade liquid nitrogen Dewar. The samples were diluted to a final concentration of $5 \mu\text{g}$ of Chl/mL using buffer containing 0.4 M sucrose, 15 mM NaCl, 5 mM MgCl_2 , and 20 mM Mes/NaOH (pH 6.0) and were excited at 436 nm. The excitation and emission slits were 5 and 2 nm, respectively. Spectra were normalized at 685 nm.

Circular dichroism spectra were recorded at 4 °C on an Aviv CD spectrometer (Model 40DS/UV–Vis–IR) provided with a circulating water bath. The bandwidth was 2 nm. The PSII RC concentrations were adjusted to $20 \mu\text{g/mL}$ Chl in buffer A. Each experiment was carried out in triplicate.

TABLE 1: Pigment Composition in Isolated WT and D1-L210H Mutant PSII Reaction Center Preparations^a

	Chl <i>a</i>	Pheo <i>a</i>
WT	6.5 ± 0.5	2 ± 0.2
D1-L210H	7.5 ± 0.5	1 ± 0.1

^a The standard deviation from four determinations is shown.

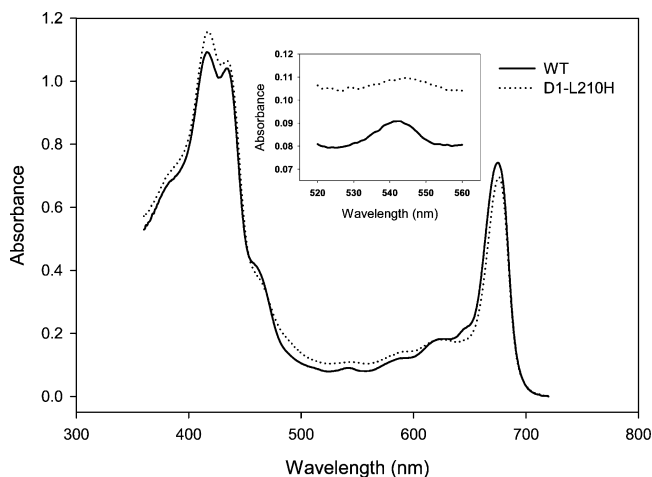


Figure 2. Room-temperature ground-state absorption spectra of PSII RCs isolated from wild-type and D1-L210H mutant strains. Spectrum for WT, —; D1-L210 mutant, ---. Inset: absorption spectra of Pheo Qx band of PSII RCs in WT and D1-L210 mutants.

Femtosecond transient absorption measurements were carried out using PSII RCs as described in ref 9. Sub-200 fs excitation pulses were centered at 685 nm, and different samples were used in the experiment to assess the reproducibility of the data. During data collection, samples (typically 40–50 μM Chl) were maintained at 4 °C and were rapidly stirred in a cuvette under anaerobic conditions.

Results

The identity of the *Chlamydomonas* D1-L210H mutant was confirmed by PCR amplification of the introduced *psb A* gene, identification of a mutation-specific, diagnostic restriction fragment length polymorphism, and DNA sequence analysis (data not shown). To determine whether the mutations altered the pigment composition of the PSII RCs, we measured the Chl and Pheo content of isolated RCs. As indicated in Table 1, WT RCs had a typical Chl/Pheo ratio of 6.5:2. In contrast, the molar ratio of Chl to Pheo was 7.5:1 in the D1-L210H mutant consistent with the replacement of one Pheo with a Chl. This interpretation was further supported by the room-temperature ground-state absorption spectra of the WT and D1-L210H mutant PSII RCs (Figure 2, inset). Consistent with the loss of one Pheo, the amplitude of the Pheo Qx absorption peak in the D1-L210H mutant was 50% less than that of WT. No apparent spectral changes were observed, however, in the Chl Qy region of WT or mutant PSII RCs (Figure 2). Notably, an apparent red shift of the Pheo Qx absorption band (~ 1.5 – 2 nm) was observed in the D1-L210H PSII RC spectra relative to WT (Figure 2, inset). The two Pheo's in PSII RCs have different absorption maxima similar to their counterparts in the BRC. The long-wavelength-absorbing form of Pheo is attributed to the Pheo $_{\text{active}}$.^{4,18,28,36} Relative to Pheo $_{\text{active}}$ the Pheo $_{\text{inactive}}$ Qx band is blue-shifted.^{37,38} The observed red shift in the Qx region of the D1-L210H RCs is attributed to the loss of blue-shifted Pheo $_{\text{inactive}}$ (539 nm).

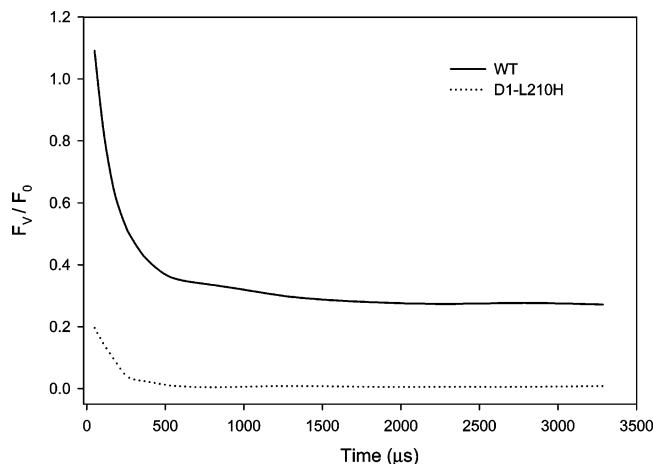


Figure 3. Chlorophyll fluorescence decay kinetics of light-grown cells from WT and D1-L210H mutant strains. WT, —; D1-L210 mutant, ---.

TABLE 2: Oxygen Evolution Rates of PSII Core Particles Isolated from WT and D1-L210H Mutant Strain^a

	O ₂ evoln rate (μ mol of O ₂ mg Chl ⁻¹ h ⁻¹)
WT	270 ± 20 (100%)
D1-L210H	10 ± 5 (3.7%)

^a Values are the average of three separate measurements using isolated PSII particles.

To determine whether the mutation affected energy and electron transfer processes in intact PSII complexes, flash-induced Chl *a* fluorescence rise and decay kinetics in dark-adapted WT and D1-L210H cells were measured. The rapid rise of Chl fluorescence from F_0 to F_M is indicative of the reduction of Q_A .³⁹ We observed a significantly reduced variable Chl *a* fluorescence yield for the D1-L210H mutant relative to WT, indicating that this mutant had a reduced ability to form the high Chl fluorescence state, $P680/Q_A^-$ (Figure 3).

Oxygen evolution rate measurements provided further evidence that electron transfer in the D1-L210H mutant was impaired. D1-L210H mutant thylakoid membranes had only 4% of the O₂-evolving activity of WT thylakoids when measured under light-saturating conditions, indicative of a block in PSII electron transfer (Table 2).

The first stable charge-separated state generated in PSII after the primary photochemical reaction is the $S_2Q_A^-$ state, representing reduction of Q_A and oxidation of the Mn-containing, water-splitting complex. As previously discussed, Chl fluorescence decay measurements following a flash of light suggested that Q_A^- was not generated in the mutant. To determine whether Q_A^- would accumulate under conditions where forward and reverse electron flow from Q_A^- were inhibited, we measured the light-induced accumulation of Q_A^- by EPR using PSII core particles at cryogenic temperatures in the presence of formate to block Q_A^- to Q_B electron transfer. Due to the magnetic interaction between Q_A^- and the nearby Fe^{2+} atom, a diagnostic EPR signal at $g = 1.82$ was generated. The yield of sodium formate enhanced $Q_A^-Fe^{2+}$ signal in the D1-L210H mutant was dramatically reduced relative to WT (Figure 4). Using Tyr_D^* as an internal standard, the integrated yield of the $Q_A^-Fe^{2+}$ signal in the mutant was determined to be only 6% that of WT.

To determine if Pheo was reduced under conditions favorable for its photoaccumulation, we measured Pheo accumulation in sodium dithionite treated PSII RC preparations illuminated at 4 °C by EPR. Figure 5 shows the light-minus-dark EPR spectra of reduced Pheo in WT and the D1-L210H mutant recorded at

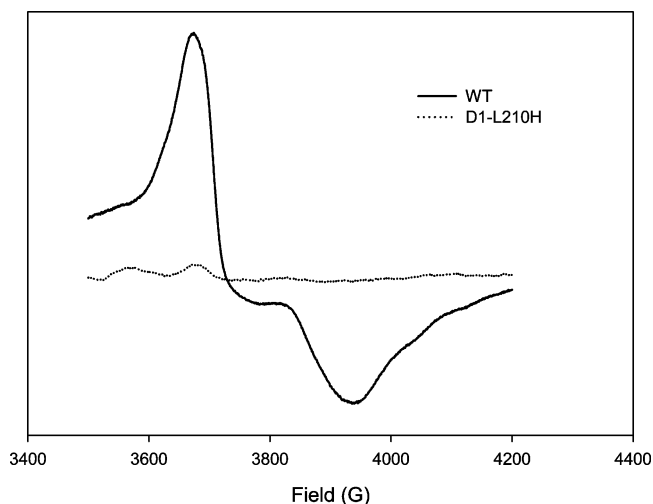


Figure 4. Sodium formate enhanced $Q_A^-Fe^{2+}$ EPR signal ($g = 1.82$ and 1.67) in PSII core particles from WT and D1-L210H mutant strains. WT, —; D1-L210 mutant, ---. EPR conditions: sample temperature, 4 K; microwave power, 32 mW; microwave frequency, 9.48 GHz; field modulation frequency, 100 kHz; magnetic field modulation amplitude, 2.0 mT. The Y-axis is relative yield of the EPR detectable radical normalized to Y_D^* .

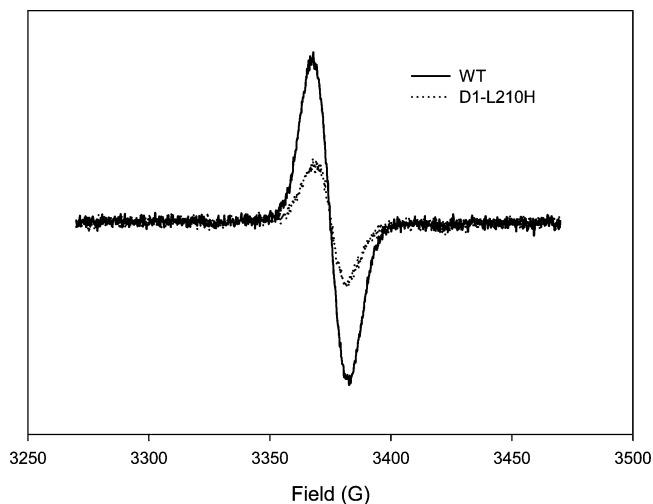


Figure 5. Photoaccumulated Pheo EPR signal in isolated PSII RCs from WT and D1-L210H mutant strains. WT, —; D1-L210 mutant, ---. The Y-axis is relative yield of the EPR detectable radical normalized to Y_D^* .

15 K. The line shape and line width of the Pheo EPR signal in the D1-L210H mutant was identical to that of WT. However, the steady-state yield of the $g = 2.003$ Pheo radical was significantly reduced in the D1-L210H mutant (approximate 25% ± 5% of WT). These results indicate a substantial reduction in either primary charge separation or an accelerated back-reaction between $Pheo^-$ and P^+ .

To determine the contributions of $Pheo^-$ to the light-minus-dark absorption spectrum of PSII RC, we compared the light-induced absorption difference spectra of wild-type and D1-L210H mutant PSII RCs. Figure 6 shows the absorption difference spectra recorded at 4 °C upon illumination for 10 s in the presence of 1 μM methyl viologen and 2.0 μg/mL sodium dithionite to reduce Pheo. The light-induced absorption difference spectrum of WT RCs resembled that seen in spinach,³⁸ with negative peaks at 515, 543, and 682 nm and positive peaks at 595 and 656 nm.^{4,41} There was a pronounced red shift in the Pheo Qx band in the D1-L210H mutant relative to WT,

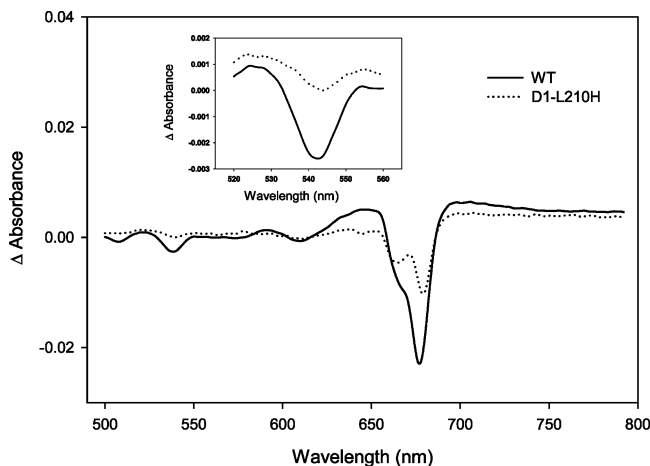


Figure 6. Light-induced absorption difference spectra of isolated PSII RCs from WT and D1-L210H mutant strains. WT, —; D1-L210 mutant, ---. Inset: spectra of Pheo Qx absorption region. PSII RCs were illuminated in the presence of methyl viologen and sodium dithionite with white actinic light ($2500 \mu\text{mol}$ of photons $\text{m}^{-2} \text{s}^{-1}$) through a heat absorbing filter for 10 s.

consistent with the loss of the blue-shifted $\text{Pheo}_{\text{inactive}}^{10}$. Considering that $\text{Pheo}_{\text{active}}$ absorbs at a longer wavelength than $\text{Pheo}_{\text{inactive}}$ (Figure 2), such results imply that both $\text{Pheo}_{\text{inactive}}$ and $\text{Pheo}_{\text{active}}$ contribute to the Pheo Qx band bleaching under continuous illumination in wild-type RCs. This bleaching could be attributed to either reduced or excited-state Pheo since both have identical spectra. In addition, there were large shifts in the Pheo Qy bands of the D1-L210H mutant at 663, 670, and

680 nm relative to WT. The Qy absorbance transitions at 670 and 681 nm have been attributed in part to Pheo and are confirmed by the absorbance differences observed in Figure 6.¹⁰

To examine the primary photochemistry of the D1-L210H mutant, we measured Pheo reduction kinetics in isolated PSII RCs at 4 °C following a series of laser flashes. Pheo^- Qx bleach kinetics were measured at two different wavelengths: 542.2 nm for WT and 543.6 nm for the D1-L210H mutant. Figure 7 shows the transient absorption kinetics in the Pheo Qx region following excitation at 685 nm. Our fits were started at 0.5 ps following the pump flash to exclude instrument-response-limited components, which presumably include buffer-associated transients as well as the simultaneous excited-state absorption of chlorins.⁹ Three exponential decay components were required to adequately fit the data (Table 3). As expected for primary charge separation, the time constant for the fastest lifetime component was 3.6 ps in WT^{9,33} and 5.2 ps in mutant RCs. Overall, there were no large differences in the lifetime components between the mutant and WT, although the τ values of the fast components fell just outside their respective error bars. However, the amplitude of the middle lifetime component (50–60 ps), attributed to energy equilibration within the RC, increased by a factor of ~ 1.5 in mutant RCs relative to WT RCs.

Figure 8 shows the Pheo^- transient absorption spectra of D1-L210H and WT PSII RCs observed 1.5 ns after a 200 nJ, 685 nm excitation pulse. These data have been normalized to 558.5 nm. The Pheo Qx bleach at 1.5 ns is attributed to the formation of charge-separated $\text{P680}^+\text{Pheo}^-$ state.⁴² At this time interval bleaching contributions from $\text{Pheo}_{\text{inactive}}$ are also maximal.¹⁰ It was apparent from analysis of the Pheo^- Qx bleach spectra of

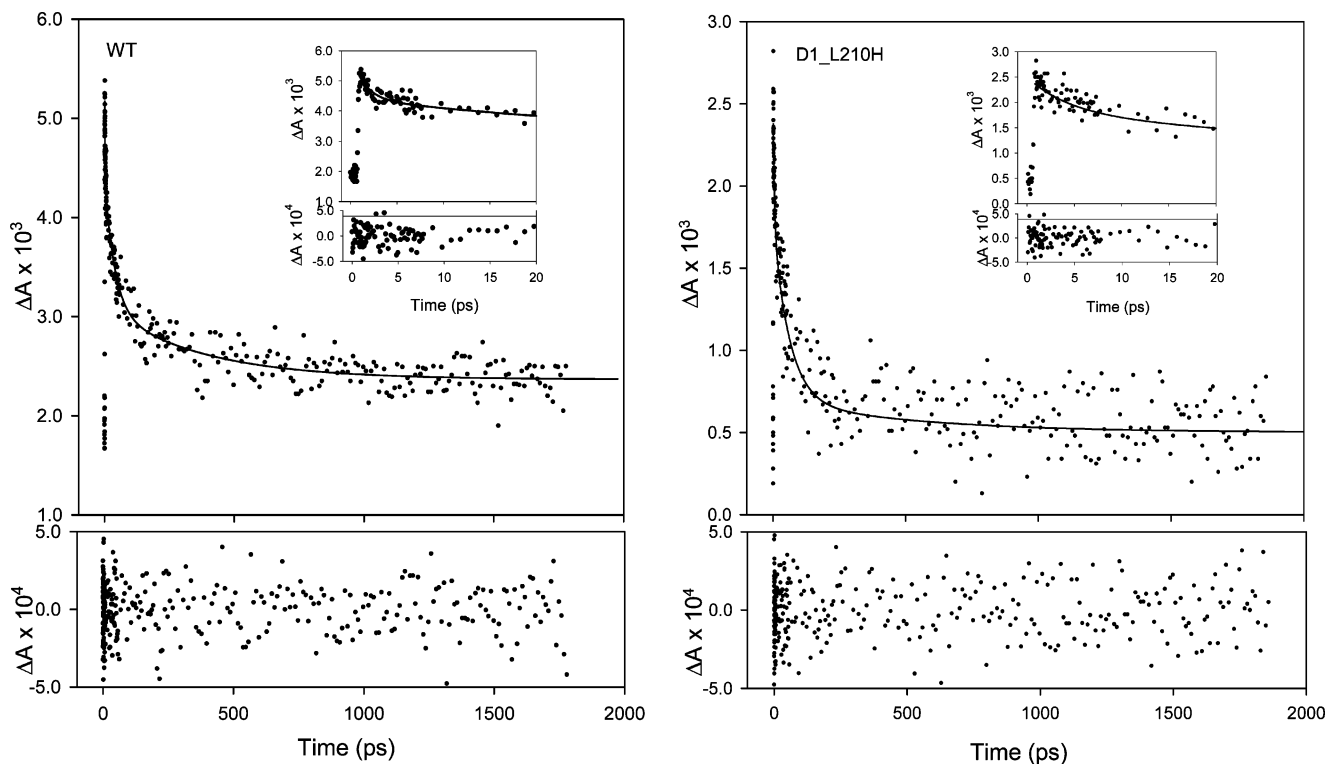


Figure 7. Transient absorption kinetics for isolated PSII RCs at 542.2 nm (WT) and 543.6 nm (D1-L210H) at 4 °C. Inset: kinetics at early time.

TABLE 3: Averages and Estimated Errors for the Fit Parameter to the Data at the Peak of the Pheo Qx Band (542.2 nm for WT and 543.6 nm for D1-L210H Mutant) in Isolated PSII Reaction Center Complex

	τ_{fast} (ps)	A_{fast} (%)	$\tau_{\text{intermediate}}$ (ps)	$A_{\text{intermediate}}$ (%)	τ_{slow} (ps)	A_{slow} (%)
WT	3.6 ± 0.5	39 ± 2	59 ± 2	38 ± 3	429 ± 10	22 ± 5
D1-L210H	5.2 ± 1	32 ± 4	62 ± 4	57 ± 5	538 ± 5	11 ± 5

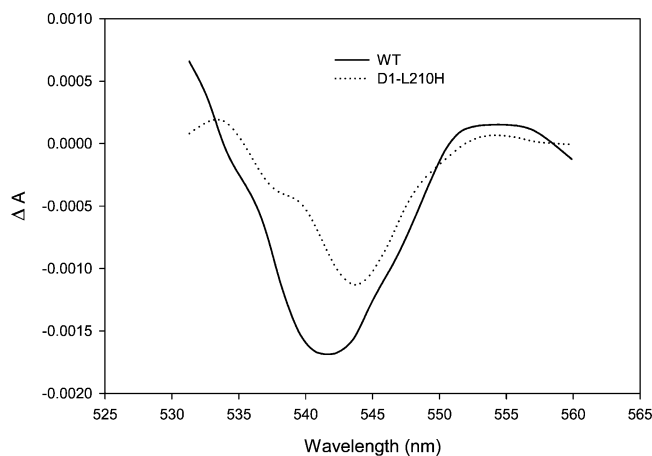


Figure 8. Transient absorption spectra of isolated PSII RCs at 4 °C recorded 1.5 ns following a 200 nJ, 685 nm excitation pulse. WT, —; D1-L210 mutant, ---.

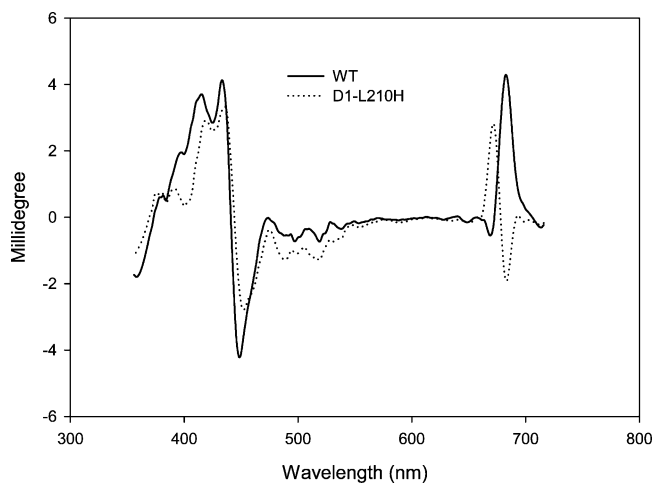


Figure 9. Visible light (4 °C) CD spectra of PSII reaction centers isolated from WT and D1-L210H mutant strains. WT, —; D1-L210 mutant, ---.

WT and the D1-L210H mutant RCs that there was no contribution from Pheo_{inactive} in the mutant. These results are consistent with the replacement of Pheo_{inactive} and not Pheo_{active} with a Chl.

To characterize energy coupling in D1-L210H mutant, we measured the Chl/Pheo CD spectra of WT and D1-L210H mutant RCs. This spectroscopic method is sensitive to pigment–pigment interactions within the PSII RC complex. Importantly, the spectra shown in Figure 9 were highly reproducible between different RC preparations. The Chl CD spectrum of WT RCs had a strong positive signal centered at 682 nm and a smaller negative peak at 669 nm. These two peaks were inverted in the D1-L210H RCs, however. The positive–negative band pair in the red region of the CD spectrum is thought to be associated with excitonic interactions involving P680, although recent studies suggest that absorbance changes at 680 nm can arise from interactions between other RC chlorins as well as contributions from pigment–protein interactions.^{43–46} Significantly, the CD and light-induced absorption spectra (Figure 6) of the D1-L210H mutant have similar changes in absorption peaks (669 and 682 nm) relative to WT. These changes presumably result from the loss of electronic interactions between Pheo_{inactive} and the RC Chl's and the addition of new electronic interactions between the Chl occupying the Pheo_{inactive} binding site and adjacent pigments. Interestingly, in RCs with Pheo_{inactive} replaced by modified Pheo (13¹-OH-Pheo), similar ΔCD peaks were

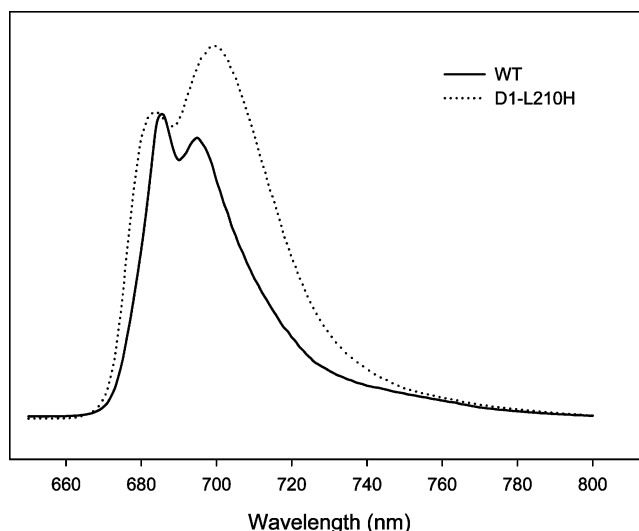


Figure 10. Chl fluorescence spectra of PSII core particles from WT and D1-L210H mutant strains at 77 K. WT, —; D1-L210 mutant, ---. The Y-axis is relative fluorescence yield normalized to 685 nm.

observed at 667 and 682 nm,²⁹ consistent with Pheo_{inactive} taking part in excitonic interactions with the other cofactors.

To characterize further the effects of replacing Pheo_{inactive} on energy transfer processes in intact PSII complexes, we measured the Chl fluorescence emission spectrum of intact PSII core particles at 77 K. These complexes contain the Chl–protein complexes of the proximal and distal antennae in addition to the reaction center complex. These measurements allow us to assess alterations in excited-state deexcitation pathways involving Chl's of the antenna complex. As shown in Figure 10, the Chl fluorescence emission spectrum of WT PSII membranes exhibits two distinct emission bands centered at 685 and 695 nm. The emission at 695 nm is attributed to a low-energy Chl bound to the H-114 residue of the proximal CP47 chlorophyll–protein antenna subunit.⁴⁷ The origin of the maximum at the 685 nm emission band is more complicated and includes contributions from charge recombination⁴⁸ and the distal light-harvesting II (LHC-II) chlorophyll–protein complex.⁴⁹ As shown in Figure 10, the D1-L210H mutant has an elevated and red-shifted Chl fluorescence emission at 699 nm (relative to the 695 nm emission peak) and a slightly blue-shifted Chl fluorescence emission at 683 nm presumably arising from the proximal antenna complex. The elevated Chl fluorescence emission in the mutant was also reflected by the high Chl fluorescence F_0 level detected in transient Chl fluorescence assays using whole cells (Figure 3 and data not shown).

Discussion

We have demonstrated that the replacement of the D1-210 leucine residue with a histidine residue resulted in the incorporation of a Chl into the Pheo_{inactive} binding site. This conclusion is based on analysis of the pigment composition of PSII RCs and the observed red shifts in the absorption spectra of both the ground state (Figure 2) and transiently reduced (Figure 8) Pheo Qx band. The mutant Pheo Qx band was red-shifted 2 nm with respect to WT (542 nm), consistent with the assignment of the blue-shifted Pheo to the inactive branch Pheo.^{10,37}

Light-saturated rates of O₂ evolution (Table 2) and the Chl fluorescence decay kinetics of PSII in cells (Figure 3) demonstrated that the D1-L210H mutant had a substantially reduced ability to carry out forward electron transfer compared to the

WT. While some reduced Pheo_{active} (30% of WT) was photoaccumulated in isolated D1-L210H RC complexes (at cryogenic temperatures), virtually no Q_A⁻ (4% of WT) accumulated in intact PSII core particles under conditions (cryogenic temperatures plus formate) in which electron transfer to Q_B was blocked. These results indicate that intact PSII preparations of the D1-L210H mutant had a substantially impaired ability to stabilize the charge-separated state. This was surprising given the fact that the Pheo not involved in charge separation was the pigment replaced by a Chl and not vice versa.

The transient absorption spectra (Figure 8) showed that the amplitude of the Pheo Q_x bleach in the isolated D1-L210H RCs (1.5 ns) was reduced (~40–50%) relative to WT. We attribute the observed Pheo bleach to the formation of the radical pair P680⁺Pheo⁻ rather than to a long-lived (1.5 ns) Pheo*. Thus, we conclude that in D1-L210H RCs the steady-state yield of radical pair formation is about half that in WT PSII RCs (Figure 6). Previously, it has been reported that one Pheo/RC is reduced under continuous illumination in the presence of dithionite and methyl viologen.⁴ However, it was not possible from these early measurements to determine which of the two Pheo's was bleached. If there were no Pheo Q_x bleaching contributions from Pheo* at 1.5 ns post excitation, then we would conclude that in WT RCs both Pheo's are reduced. Jankowiak et al.¹⁰ demonstrated, however, that both Pheo_{active} and Pheo_{inactive} were bleached in WT PSII RCs. The kinetics of Pheo_{inactive} bleaching, however, were much slower than those for Pheo_{active}. At early times (<10 ps) the Pheo Q_x bleach is dominated by Pheo_{active}, but by 1.5 ns it is dominated by Pheo_{inactive} bleaching. They attributed the slow bleaching of Pheo_{inactive} to energy equilibration between higher delocalized Q_y states and the Pheo_{inactive} Q_y state following relaxation of the Pheo_{active} Q_x state. We favor this explanation for the bleaching of Pheo_{inactive} in WT RCs.

In the D1-L210H mutant increased occupancy of the Chl, which replaced Pheo_{inactive}, by the lowest excited state could account for both the reduced quantum yield of charge separation and the increased Chl fluorescence from PSII core particles. In support of this interpretation, it is clear from the Chl CD spectra of WT and D1-L210H RCs (Figure 9) that there were substantial changes in the excitonic interactions between pigments in D1-L210H RCs. The Pheo Q_y CD features (670 and 681 nm) of the D1-L210H mutant have the appearance of a derivative spectrum relative to WT. Such spectra may result from altered phase interactions between the multiple components of the delocalized excited states across the six core chlorins and are consistent with a redistribution of the excited-state equilibrium among the pigments of the multimer.

Theoretically, it has been shown that the small orbital energy shifts belonging to one pigment relative to that of another can give rise to significant effects on the electronic coupling matrix elements for electron transfer.⁵⁰ The presence of Mg in the Chl changes the distribution of electrons in the highest occupied and lowest unoccupied molecular orbitals. This results in a change in the overall electronic structure of the Chl excited state, which in turn is reflected in the electronic coupling between the Chl and the remaining pigments within the multimer complex. We observed a distinct narrowing of the Chl fluorescence of mutant PSII RCs relative to WT (data not shown) consistent with a stronger coupling between pigments of the mutant PSII RC relative to WT. Given the increased and distinctly blue-shifted Chl fluorescence emission arising from the proximal antennae and substantially increased and red-shifted Chl fluorescence emission from the distal antenna complexes (Figure 10) of D1-L210H PSII core particles, we propose that

there is an increased occupancy of inactive branch pigments by the lowest excited state. In mutant PSII core particles, the excited state is then dissipated via new deexcitation networks ultimately leading to reductions in the yield of charge-separated states (Table 2, Figures 2–6, 8) and increased yields of Chl fluorescence (Figure 10).

Acknowledgment. Work at NREL was supported by the Division of Energy Biosciences, Office of Basic Energy Sciences, US Department of Energy under Contract No. DE-AC36-99G010337. Work at the Ohio State University (R.T.S.) was supported under subcontract through NREL. Work at Northwestern was supported by the Division of Chemical Sciences, Office of Basic Energy Sciences, US Department of Energy under Grant DE-FG02-99ER14999.

References and Notes

- (1) Seibert, M. In *The Photosynthetic Reaction Center*; Deisenhofer, J., Norris, J. R., Eds.; Academic Press: Orlando, 1993; Vol. I, pp 319–356.
- (2) Diner, B. A.; Rappaport, F. *Annu. Rev. Plant Biol.* **2002**, *53*, 551–80.
- (3) Allen, J. P.; Williams, J. C. *FEBS Lett.* **1998**, *438*, 5–9.
- (4) Nanba, O.; Satoh, K. *Proc. Natl. Acad. Sci. U.S.A.* **1987**, *84*, 109–112.
- (5) Rhee, K.-H.; Morris, E. P.; Barber, J.; Kühlbrandt, W. *Nature* **1998**, *396*, 283–286.
- (6) Zounl, A.; Witt, H.-T.; Kern, J.; Fromme, P.; Kraub, N.; Saenger, W.; Orth, P. *Nature* **2001**, *409*, 739–743.
- (7) Kirmaier, C.; Holten, D. *The photosynthetic reaction center*; Academic Press: San Diego, 1993; Vol. II.
- (8) Klimov, V. V.; Dolan, E.; Ke, B. *FEBS Lett.* **1980**, *112*, 97–100.
- (9) Greenfield, S. R.; Seibert, M.; Govindjee, Wasielewski, M. R. *J. Phys. Chem. B* **1997**, *101*, 2251–2255.
- (10) Jankowiak, R.; Hayes, J. M.; Small, G. J. *J. Phys. Chem. B* **2002**, *106*, 8803–8814.
- (11) Van Grondelle, R.; Dekker, J. P.; Gillbro, T.; Sundström, V. *Biochim. Biophys. Acta* **1994**, *1187*, 1–65.
- (12) Rutherford, A. W.; Aterson, D. R.; Mullet, J. E. *Biochim. Biophys. Acta* **1981**, *635*, 205–214.
- (13) Konermann, L.; Holzwarth, A. R. *Biochemistry* **1996**, *35*, 829–842.
- (14) Peterman, E. J. G.; van Amerongen, H.; van Grondelle, R.; Dekker, J. P. *Proc. Natl. Acad. Sci. U.S.A.* **1998**, *95*, 6128–33.
- (15) Dekker, Jan. P.; van Grondelle, R. *Photosyn. Res.* **2000**, *63*, 195–208.
- (16) Noguchi, T.; Tomo, T.; Kato, C. *Biochemistry* **2001**, *40*, 2176–2185.
- (17) Durrant, J. R.; Klug, D. R.; Kwa, S. L. S.; Grondelle, R. V.; Porter, G.; Dekker, J. P. *Proc. Natl. Acad. Sci. U.S.A.* **1995**, *92*, 4798–4802.
- (18) Tetenkin, V. L.; Gulyaev, B. A.; Seibert, M.; Rubin, A. *FEBS Lett.* **1989**, *20*, 459–463.
- (19) Kirmaier, C.; Holten, D. *Photosynth. Res.* **1987**, *13*, 225–260.
- (20) Kirmaier, C.; Holten, D.; Bylina, E. J. *Proc. Natl. Acad. Sci. U.S.A.* **1988**, *85*, 7562–7566.
- (21) Kirmaier, C.; Gaul, D.; DeBey, R.; Holten, D.; Schenck, C. C. *Science* **1991**, *251*, 922–927.
- (22) Heller, B. A.; Holten, D.; Kirmaier, C. *Science* **1995**, *269*, 940–945.
- (23) Lin, S.; Jackson J. A.; Taguchi, A. K. W.; Woodbury, N. W. *Biochemistry* **1999**, *103*, 4757–4763.
- (24) Lin, S.; Katilius, E.; Haffa, A. L. M.; Taguchi, A. K. W.; Woodbury, N. W. *Biochemistry* **2001**, *40*, 13767–13773.
- (25) Allen, J. P.; Artz, K.; Lin, X.; Mattioli, T. A. *Biochemistry* **1996**, *35*, 6612–6619.
- (26) Chirino, A. J.; Lous, E. J.; Huber, M.; Allen, J. P.; Schenck, C. C.; Paddock, M. L.; Feher, G.; Ress, D. C. *Biochemistry* **1994**, *33*, 4584–4593.
- (27) Gall, B.; Zehetner, A.; Scherz, A.; Sheer, H. *FEBS Lett.* **1998**, *434*, 88–92.
- (28) Shkuropatov, A. Y.; Khatypov, R. A.; Shkuropatova, V. A.; Zvereva, M. G.; Owens, T. G.; Shuvalov, V. A. *FEBS Lett.* **1999**, *450*, 163–167.
- (29) Germano, M.; Shkuropatov, A. Ya.; Permentier, H.; de Wijn, R.; Hoff, A. J.; Shuvalov, V. A.; van Gorkom, H. J. *Biochemistry* **2001**, *40*, 11472–11482.
- (30) Germano, M.; Pascal, A.; Shkuropatov, A. Ya.; Robert, B.; Hoff, A. J.; van Gorkom, H. J. *Biochemistry* **2002**, *41*, 11449–1145.

- (31) Minagawa, J.; Crofts, A. R. *Photosynth. Res.* **1994**, *42*, 121–131.
- (32) Roffey, R. A.; Golbeck, J. H.; Hille, C. R.; Sayre, R. T. *Biochim. Biophys. Acta* **1994**, *1185*, 257–270.
- (33) Wang, J.; Gosztola, D.; Ruffle, S. T.; Hemann, C.; Seibert, M.; Wasielewski, M.; Hille, R.; Gustafson, T. L.; Sayre, R. T. *Proc. Natl. Acad. Sci. U.S.A.* **2002**, *99*, 4091–4096.
- (34) Eijkelhoff, C.; Dekker, J. P. *Photosynth. Res.* **1997**, *52*, 69–73.
- (35) Kramer, D. M.; Robinson, H. R.; Crofts, A. R. *Photosynth. Res.* **1990**, *26*, 181–193.
- (36) Van der Vo, R.; van Leeuwen, P. J.; Braun, P.; Hoff, A. J. *Biochim. Biophys. Acta* **1992**, *1140*, 184–198.
- (37) Mimuro, M.; Tomo, T.; Nishimura, Y.; Yamazaki, I.; Satoh, K. *Biochim. Biophys. Acta* **1995**, *1232*, 81–88.
- (38) Jankowiak, R.; Rätsep, M.; Picorel, R.; Seibert, M.; Small, G. J. *J. Phys. Chem. B* **1999**, *103*, 9759–9769.
- (39) Philbrick, J. B.; Diner, B. A.; Zilinskas, B. A. *J. Biol. Chem.* **1991**, *266*, 13370–13376.
- (40) Yruela, I.; Torrado, E.; Roncel, M.; Picorel, R. *Photosynth. Res.* **2001**, *67*, 199–206.
- (41) Yruela, I.; van Kan, P. J. M.; Müller, M. G.; Holzwarth, A. R. *FEBS Lett.* **1994**, *339*, 25–30.
- (42) Greenfield, S. R.; Seibert, M.; Wasielewski, M. R. *J. Phys. Chem. B* **1999**, *103*, 8364–8374.
- (43) Tang, X.-S.; Fushimi, K.; Satoh, K. *FEBS Lett.* **1990**, *273*, 257–260.
- (44) Finzi, L.; Elli, G.; Cucchelli, G.; Garlaschi, F. M.; Jennings, R. C. *Biochim. Biophys. Acta* **1998**, *1366*, 256–264.
- (45) Finzi, L.; Zucchelli, G.; Garlaschi, F. M.; Jennings, R. C. *Biochemistry* **1999**, *38*, 10627–10631.
- (46) Vacha, F.; Dürchan, M.; Siffel, P. *Biochim. Biophys. Acta* **2002**, *1554*, 147–152.
- (47) Shen, G.; Vermass, W. F. J. *Biochemistry* **1994**, *33*, 7379–7388.
- (48) Braun, P.; Greenberg, B. M.; Scherz, A. *Biochemistry* **1990**, *29*, 10376–10387.
- (49) Funk, C.; Schröder, W. P.; Salih, G.; Wiklund, R.; Jansson, C. *FEBS Lett.* **1998**, *436*, 434–438.
- (50) Scherer, P. O. J.; Fischer, S. F. *J. Phys. Chem.* **1989**, *93*, 1633–1637.
- (51) Abbreviations: BChl, bacteriochlorophyll; BPheo, bacterial pheophytin; P, primary donor; BRC, bacterial reaction center; Chl, chlorophyll; Chl_M, chlorophyll monomer; Chl_{SP}, chlorophyll special pair; Pheo, pheophytin; Pheo_{active}, active branch pheophytin; Pheo_{inactive}, inactive branch pheophytin; PSII, photosystem II; Q_A, plastoquinone binding site A; Q_B, plastoquinone binding site B; P680, primary donor of photosystem II; RC, reaction center; TAP, Tris–acetate–phosphate growth media; WT, wild type.